Optics Letters

Raman dissipative soliton fiber laser pumped by an ASE source

Weiwei Pan,[1,2] Lei Zhang,[1,3] Jiaqi Zhou,[1,4] Xuezong Yang,[1,2] and Yan Feng[1,*]

[1]Shanghai Institute of Optics and Fine Mechanics, Chinese Academy of Sciences, and Shanghai Key Laboratory of Solid State Laser and Application, Shanghai 201800, China
[2]University of the Chinese Academy of Sciences, Beijing 100049, China
[3]e-mail: zhangl@siom.ac.cn
[4]e-mail: jqzhou@siom.ac.cn
*Corresponding author: feng@siom.ac.cn

Received 13 October 2017; revised 11 November 2017; accepted 13 November 2017; posted 14 November 2017 (Doc. ID 309046); published 8 December 2017

The mode locking of a Raman fiber laser with an amplified spontaneous emission (ASE) pump source is investigated for performance improvement. Raman dissipative solitons with a compressed pulse duration of 1.05 ps at a repetition rate of 2.47 MHz are generated by utilizing nonlinear polarization rotation and all-fiber Lyot filter. A signal-to-noise ratio as high as 85 dB is measured in a radio-frequency spectrum, which suggests excellent temporal stability. Multiple-pulse operation with unique random static distribution is observed for the first time, to the best of our knowledge, at higher pump power in mode-locked Raman fiber lasers.

OCIS codes: (140.3510) Lasers, fiber; (140.3550) Lasers, Raman; (140.4050) Mode-locked lasers.

https://doi.org/10.1364/OL.42.005162

In the past two decades, ultrafast fiber lasers have been extensively studied for various applications in fundamental research, biomedicine, and industry [1–3]. Usually, ultrafast fiber lasers use rare-earth-doped fibers as gain media, which enjoy the advantages of high gain and broad gain bandwidth. However, they also suffer from the disadvantage of limited working spectral regions. In comparison, Raman fiber lasers use stimulated Raman scattering (SRS) to provide gain, which has the advantages of wavelength agility and broad gain bandwidth [4,5]. By using Raman fibers as the gain medium instead of rare-earth-doped fibers in ultrafast fiber lasers, wavelength-agile ultrashort pulses can be obtained with appropriate pump laser and optical components, which can effectively extend the application fields of ultrafast fiber laser.

Ultrafast Raman fiber lasers with continuous-wave (CW) pumps and various mode-locking techniques have been investigated, including passive methods with saturable absorbers [6,7] and equivalent saturable absorbers [8,9], and active ones with intra-cavity modulators [10] and hybrid mode-locking techniques [11]. As the rare-earth-doped ones, ultrafast Raman fiber lasers are also robust and compact. Nevertheless, their characteristics such as pulse energy, pulse width, and stability of the pulse train are worse than the rare-earth-doped counterparts. That is due to the fact that a long piece of Raman fiber is usually needed under a CW pump which, on the other hand, increases the accumulation of nonlinearity and dispersion to consequently deteriorate pulse-train and stretch pulses. Furthermore, SRS is a nonlinear effect with response time in the level of femtoseconds. The temporal characteristic of the pump laser would be transferred to the Raman light, together with the power conversion. A pump laser with poor temporal stability would also exacerbate the performance of a mode-locked Raman fiber laser.

An ultrafast Raman laser can also be generated under synchronously pulse pumping [12,13]. Due to the high peak power of the pump pulse, a piece of Raman fiber that is only several meters in length can provide enough gain to overcome loss. Thus, overall output performances of synchronously pumped Raman fiber lasers are better than those under the CW pump. However, in synchronous pumping, the cavity lengths of the pump and Raman laser must be adjusted to match each other [12]. Both lengths may drift in practice due to temperature variation and mechanical vibration, which results in excessive noise in the output. Accurate synchronization can only be achieved by adjusting the pump repetition rate or laser cavity length in real time with a feedback control loop, which greatly increases volume and complexity of the laser system.

In ultrashort pulse generation, dissipative soliton (DS) mode locking is a valid technique to improve pulse stability. Compared with the solution family of solitons in the Hamiltonian system, the DS solution is a unique and fixed solution on account of the dynamical balance among gain, loss, nonlinearity, and dispersion in a dissipative system, which leads to a more stable state in the cavity [2]. Therefore, the overall performance of ultrafast Raman fiber lasers can be improved by utilizing DS mode locking. Raman dissipative solitons (RDSs) were first reported by Castellani *et al.* in an ultrafast Raman laser mode-locked by nanotubes, but the temporal stability

Corrected 13 December 2017

is low [7]. Recently, RDS with 5 nJ of pulse energy from a synchronously pumped fiber laser was reported, in which the ytterbium pump laser and Raman laser shared a common oscillator [13]. In another demonstration, a Raman fiber laser synchronously pumped by a picosecond fiber laser can produce RDS pulses at a direct out power of 0.76 W with a conversion efficiency of 88% and a pulse width of 8 ps [12].

In this Letter, we report a high-performance RDS fiber laser pumped by a CW amplified spontaneous emission (ASE) source with high power stability. A nonlinear polarization rotation (NPR) technique is used to provide an artificial saturable absorption effect to achieve mode locking. An all-fiber Lyot filter is formed in the cavity to shape the spectrum and pulse so that RDS mode locking can be activated and stabilized. RDS pulses with a compressed pulse width of 1.05 ps and a repetition rate of 2.47 MHz are obtained. The signal-to-noise ratio (SNR) of the radio-frequency (RF) spectrum is measured to be as high as 85 dB, which suggests excellent temporal stability. In addition, unique multi-pulse RDS with random static distribution is observed at higher pump power.

The experimental setup of the RDS fiber laser is illustrated in Fig. 1. The Raman laser has a ring cavity. An ASE source at 1064 nm with high temporal stability is used as the pump source to generate a stable Raman laser. Backward pumping is adopted to improve conversion efficiency, suppress noise, and get pure Raman laser output. WDM1 and WDM2 are both 1064/1120 nm wavelength division multiplexers (WDMs), which are used to couple the pump laser into the cavity and remove the residual pump after the Raman fiber, respectively. A piece of 70 m Raman fiber (OFS Raman Fiber) is adopted to act as the Raman gain medium. A polarization-dependent (PD) isolator is used to ensure unidirectional light propagation and works as a polarizer. Two polarization controllers (PCs) that locate at either side of the isolator form a typical NPR structure together with the isolator. A short piece of PM980 fiber is spliced with the input or output PM fiber of the isolator at an angle of 45°, which works with the PD isolator to act as an all-fiber Lyot filter. A 40/60 fiber coupler is used to extract the Raman laser from the cavity, of which the 40% port is the output. The length of the cavity is about 80 m. The total group velocity dispersion in the fiber ring is about 1.6 ps^2. The whole laser setup is all-fiber connected.

The pump laser is an amplified ytterbium fiber ASE source. In order to optimize the Raman gain at 1120 nm, an ASE seed is spectrally filtered by a 10 nm bandpass filter and a 1 nm bandpass filter, successively. Then the ASE source is scaled up by two fiber amplifiers. The output power of the ASE source is up to 5.5 W. The spectrum of the ASE source at a power of

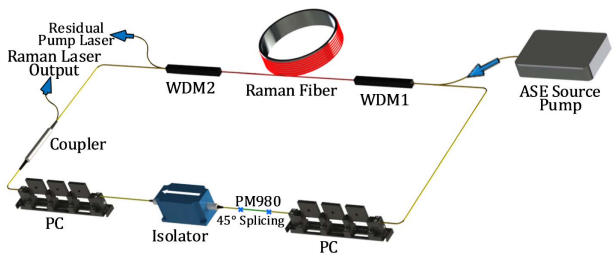

Fig. 1. Experimental setup of the laser system. WDM, wavelength division multiplexer; PC, polarization controller.

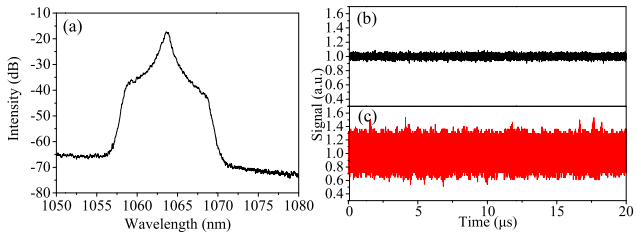

Fig. 2. (a) Spectral and (b) temporal measurements of the ASE source at an output power of 4.8 W, and (c) intensity dynamics of a fiber oscillator.

4.8 W is shown in Fig. 2(a). The spectral shape of a narrow spike on a wide pedestal is resulted from the low extinction ratio of the 1 nm bandpass filter, which has a typical value of 23 dB. Figure 2(b) presents intensity dynamics of the ASE source at the power of 4.8 W, measured with a InGaAs detector of 150 MHz bandwidth. The ASE source has much lower intensity fluctuation compared to a usual fiber laser pump source. Usual oscillator-based fiber lasers have much higher intensity fluctuation due to the longitudinal mode beating and optical nonlinearity. The intensity fluctuation of the ASE source is 2.3% in root-mean-square (RMS). The fiber oscillator used for comparison has a similar spectral linewidth and output power, which has been used to pump a tunable random Raman fiber laser [14]. The intensity dynamics of the fiber oscillator are presented in Fig. 2(c) which shows a RMS fluctuation of 28.6%. As mentioned previously, a temporal characteristic of the pump laser would be transferred to the Raman laser by SRS. In our experiments, stable RDS mode locking cannot be obtained using the fiber oscillator as a pump source. The ASE pump source plays a crucial role in generating temporally stable RDS mode locking. The ASE source from rare-earth-doped fiber has been proved to have good temporal stability [15], which is an ideal pump source for a Raman fiber laser [16]. It has been reported that high time domain stability could be obtained in a random distributed feedback Raman fiber laser under ASE source pumping [17]. However, this is the first time, to the best of our knowledge, that an ASE source is proposed to pump a mode-locked Raman fiber laser in order to improve the pulse stability.

It is well-known that spectral filtering is necessary for spectral and pulse shaping to achieve DS mode locking [2]. All-fiber Lyot filter with the advantages of high flexibility, easy implementation, and robust operation has been used in DS mode-locked fiber lasers [18]. In the laser setup, the input fiber of the PD isolator is spliced with the short PM fiber segment at an angle of 45°. A Lyot filter is formed due to the birefringence and dispersion of the PM fiber. The overall transmission of the Lyot filter, T, can be expressed as $\cos^2(\pi L\Delta n/\lambda)$ [19], where L is length of the PM fiber segment, Δn is the birefringence of the PM fiber, and λ is the wavelength of the light. The equation of T shows that the transmission spectrum is quasi-periodic with a free spectral range (FSR) given by $\Delta\lambda \sim \lambda^2/(L\Delta n)$ [20]. Thus, the length of the PM fiber segment determines the bandwidth of the Lyot filter. In the cavity, the length of the PM fiber segment is 20 cm. Taking the birefringence $\Delta n = 6.5 \times 10^{-4}$ into consideration, the FSR of the Lyot filter is about 10 nm and corresponding bandwidth of the periodic passbands is about 5 nm.

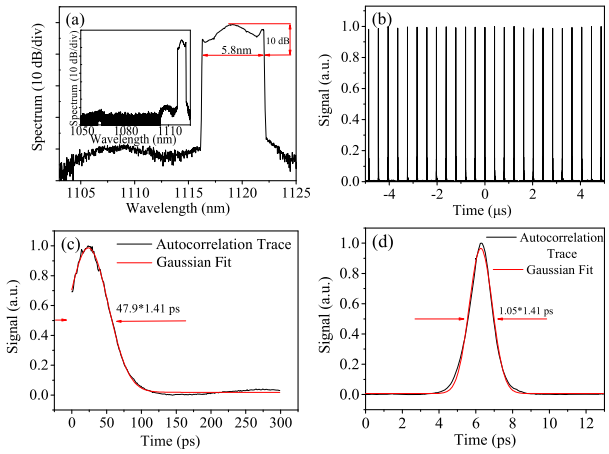

Fig. 3. Properties of the fundamental RDS pulses. (a) Spectrum; the inset is the spectrum plotted over a wider range. (b) Pulse train, and autocorrelation traces with Gaussian function fitting (c) before and (d) after (d) compression.

In the experiment, the Raman laser reaches threshold at a pump power of 4.18 W and emits a CW laser first. Further increasing the pump power and adjusting the PCs, different states of mode locking can be obtained. Fundamental RDS mode locking with a pulse energy of 0.69 nJ is obtained at a pump power of 4.73 W. Figure 3(a) plots the spectrum of the RDS pulses, which was recorded by an optical spectrum analyzer (Yokogawa, AQ6370D) at a resolution of 0.02 nm. The central wavelength is located at 1119 nm, and the 10 dB bandwidth is about 5.8 nm. The steep edge of the spectrum is typical for DS mode locking. Note the steep edge is as high as 35 dB, which suggests the high quality of the DS operation. On the blue side of the RDS spectrum, a small uplift can be observed at about 1109 nm, which originates from the nearby passband of the Lyot filter and is restrained by the main RDS peak. The inset of Fig. 3(a) plots the spectrum of the RDS pulses in a larger range. Hardly any pump laser at 1064 nm is outputted together with the Raman laser, which suggests a spectrally clean ultrashort Raman pulse output.

Figure 3(b) shows a typical mode-locked pulse train that is generated with this RDS fiber laser. The pulse train was measured by an oscilloscope of 2.5 GHz bandwidth (Keysight, DSO-S 254A) and an InGaAs detector with a bandwidth of 1.2 GHz (Thorlabs, DET010CFC). The pulse spacing of 405 ns corresponds to a repetition rate of 2.47 MHz, matching the cavity length of about 80 m. An autocorrelation trace of the RDS pulses measured by an autocorrelator (APE PulseCheck, SM1200) with a scanning range of 300 ps is shown in Fig. 3(c). Due to the scanning characteristic of the autocorrelator, only the right part of the signal can be recorded in the 300 ps scan. The width of the RDS pulse is estimated to be about 48 ps by fitting with a Gaussian function. The highly chirped RDS pulses are compressed to about 1.05 ps with a grating pair, as shown in Fig. 3(d). The pulse duration is not yet spectrally limited. Further compressing is constrained by the experiment condition.

RF characteristics of the Raman laser were analyzed with a RF spectrum analyzer with a bandwidth of 20 GHz (Keysight, N9020A) and an InGaAs detector of 150 MHz bandwidth

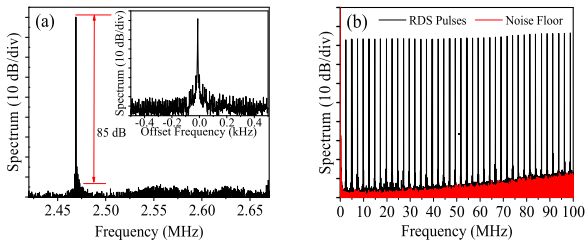

Fig. 4. RF spectra of the RDS pulses around the (a) fundamental repetition rates and (b) harmonics. Inset of (a): RF spectrum around the fundamental repetition rates in a narrower range.

(Thorlabs, PDA10CF). Figure 4(a) shows a RF spectrum of the fundamental RDS pulses around the pulse repetition rate at a resolution of 10 Hz. The SNR of the narrow spectral peak is as high as 85 dB. In the inset of Fig. 4(a), an RF spectrum with 1 Hz resolution in a range of 1 kHz is plotted, which shows an SNR of 70 dB. Figure 4(b) presents a RF spectrum up to 100 MHz at a resolution of 100 Hz, which contains a comb of the harmonics of the fundamental repetition rate. The ultrahigh SNR is maintained at high harmonics. The baseline of the harmonic comb has a lift at the high frequency end, which is due to the noise floor of the detector [also shown in Fig. 4(b)]. The ultrahigh SNR of the RF spectra suggests excellent temporal stability of the RDS pulses, which shall be attributed to the high power stability of the ASE pump source, the filtering effect of the Lyot filter and the DS mechanism.

At higher pump power ranging from 5.11 to 5.47 W, a multi-pulse RDS operation was observed. Figure 5(a) shows a pulse train at a pump power of 5.21 W which contains 23 pulses. For clarity, the pulse train is plotted by stacking the waveforms of consecutive cavity round-trips. The cavity round-trip time is 405 ns, and 20 periods are shown in the figure. It is found that the pulses are in a random, but static, distribution over the whole cavity. A similar phenomenon was observed in rare-earth-doped soliton fiber lasers [21], which

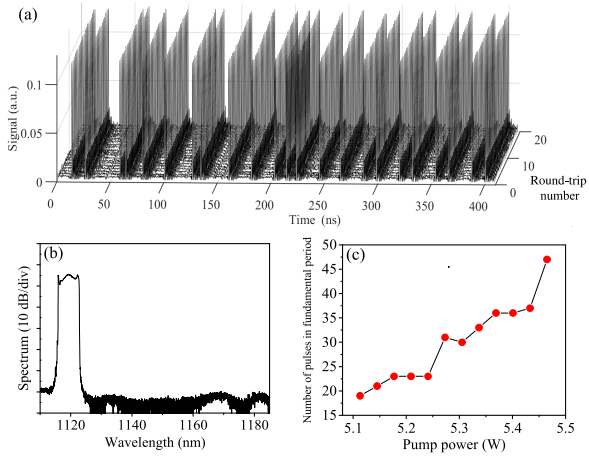

Fig. 5. Properties of the multi-pulse RDS: (a) pulse train plotted by stacking the waveforms of 20 consecutive cavity round trips and (b) output spectrum at a pump power of 5.21 W. (c) Number of pulses as a function of the pump power.

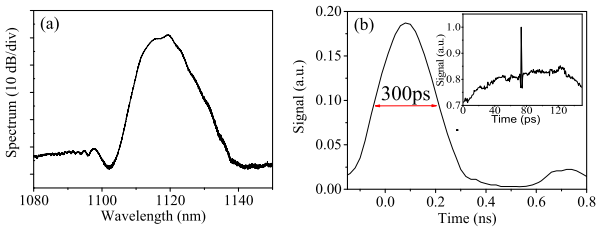

Fig. 6. (a) Spectrum and (b) pulse envelope of the mode-locked output without the Lyot filter. Inset of (b): autocorrelation trace of the output which suggests the noise-like mode locking.

likely resulted from soliton energy quantization and various soliton interactions [22,23]. Such random, but static, distribution of multi-pulse operation is observed for the first time, to the best of our knowledge, in DS mode locking and in a mode-locked Raman fiber laser.

A spectrum of the multi-pulse RDS is presented in Fig. 5(b), which still has typical DS features. Also shown in Fig. 5(b), there is no second Raman stokes laser generated. The pulse split should be caused by excess nonlinear accumulation of the pulses in the laser cavity. In the Raman cavity, the major part is the 70 m long Raman fiber. Its nonlinear index is estimated to be about five times larger than normal single-mode fiber at the 1 μm band. It can provide higher Raman gain but, on the other hand, exacerbate the accumulation of nonlinearity. Therefore, although in DS mode locking, the pulses are still likely to split at high pump power. A number of pulses are plotted against the pump power in Fig. 5(c). The pulse number tends to increase with the pump power as usual multi-pulse fiber lasers. A maximum of 47 pulses is observed. At different pump powers, the distribution of pulses is always random and static. It seems there is no interaction between the RDS pulses to either push or pull each other. A detailed understanding of the observation requires further investigation and, more importantly, detailed simulation.

The Lyot filter is the key component to achieve RDS mode locking in the Raman laser. In order to verify it, a ring cavity without Lyot filter was investigated as well. By finely and carefully adjusting the PCs at different pump powers, only a type of wide-spectrum mode locking could be obtained. The spectrum of the mode-locked output is shown in Fig. 6(a). Figure 6(b) presents the pulse envelope of the mode-locked pulses in a time domain, which was measured by a 6 GHz oscilloscope (Tektronix, DPO 90604c) with a 25 GHz InGaAs-based detector (New Focus, 1414-50). The measured pulse width is about 300 ps, while its autocorrelation trace at a range of 150 ps exhibits a narrow spike at the middle [inset of Fig. 6(b)], which suggests the mode-locked output at this condition is noise like. The noise-like mode locking is caused by the high nonlinear index of the Raman fiber and long cavity. This observation proves that the insertion of the all-fiber Lyot filter has efficiently improved the performance of the mode-locked Raman fiber laser by changing the state from noise-like mode locking to DS mode locking.

In conclusion, we have demonstrated a high-performance RDS fiber laser pumped by an ASE source. An NPR technique and all-fiber in-cavity Lyot filter are adopted to achieve stable RDS mode locking. Typical RDS pulses with steep-edge spectra are obtained. The pulse width of the RDS before and after compression is 48 and 1.05 ps, respectively. The repetition rate of the RDS is 2.47 MHz. The RF spectral SNR of the RDS pulses is as high as 85 dB, which suggests excellent temporal stability. The ultrahigh stability is enabled by the ASE pump source, which is temporally more stable than usual laser pump sources. Interesting multi-pulse RDS with a random static distribution is observed at higher pump power for the first time, to the best of our knowledge. A synchronously pumped Raman fiber laser can also generate RDS pulses, but the present CW pumped laser has lower complexity and demonstrates better noise property. In future work, a detailed numerical simulation would be very helpful in understanding the observation and further improving the wavelength-agile ultrafast Raman fiber lasers.

Funding. National Natural Science Foundation of China (NSFC) (61378026, 61505229, 61575210).

REFERENCES

1. M. E. Fermann and I. Hartl, Nat. Photonics **7**, 868 (2013).
2. P. Grelu and N. Akhmediev, Nat. Photonics **6**, 84 (2012).
3. C. Kerse, H. Kalaycıoğlu, P. Elahi, B. Çetin, D. K. Kesim, Ö. Akçaalan, S. Yavaş, M. D. Aşık, B. Öktem, and H. Hoogland, Nature **537**, 84 (2016).
4. L. Zhang, H. Jiang, S. Cui, J. Hu, and Y. Feng, Laser Photon. Rev. **8**, 889 (2014).
5. E. M. Dianov, J. Lightwave Technol. **20**, 1457 (2002).
6. L. Zhang, G. Wang, J. Hu, J. Wang, J. Fan, J. Wang, and Y. Feng, IEEE Photon. J. **4**, 1809 (2012).
7. C. E. S. Castellani, E. J. R. Kelleher, J. C. Travers, D. Popa, T. Hasan, Z. Sun, E. Flahaut, A. C. Ferrari, S. V. Popov, and J. R. Taylor, Opt. Lett. **36**, 3996 (2011).
8. A. Chamorovskiy, A. Rantamäki, A. Sirbu, A. Mereuta, E. Kapon, and O. G. Okhotnikov, Opt. Express **18**, 23872 (2010).
9. D. A. Chestnut and J. R. Taylor, Opt. Lett. **30**, 2982 (2005).
10. X. Yang, L. Zhang, H. Jiang, T. Fan, and Y. Feng, Opt. Express **23**, 19831 (2015).
11. A. G. Kuznetsov, D. S. Kharenko, E. V. Podivilov, and S. A. Babin, Opt. Express **24**, 23872 (2016).
12. D. Churin, J. Olson, R. A. Norwood, N. Peyghambarian, and K. Kieu, Opt. Lett. **40**, 2529 (2015).
13. S. A. Babin, E. V. Podivilov, D. S. Kharenko, A. E. Bednyakova, M. P. Fedoruk, V. L. Kalashnikov, and A. Apolonski, Nat. Commun. **5**, 5653 (2014).
14. L. Zhang, H. Jiang, X. Yang, W. Pan, S. Cui, and Y. Feng, Sci. Rep. **7**, 42611 (2017).
15. J. Xu, L. Huang, J. Leng, H. Xiao, S. Guo, P. Zhou, and J. Chen, Opt. Express **23**, 5485 (2015).
16. B. Levit, A. Bekker, V. Smulakovsky, and B. Fischer, *Convention of Electrical and Electronics Engineers in Israel* (2008), pp. 563–565.
17. J. Xu, P. Zhou, J. Leng, J. Wu, and H. Zhang, Sci. Rep. **6**, 35213 (2016).
18. X. Yang, L. Zhang, Y. Feng, X. Zhu, R. A. Norwood, and N. Peyghambarian, J. Lightwave Technol. **34**, 4266 (2016).
19. Z. Yan, K. Zhou, A. Adedotun, and L. Zhang, *Advanced Photonics Congress* (2012), paper BW2E.2.
20. K. Özgören and F. Ö. Ilday, Opt. Lett. **35**, 1296 (2010).
21. Y. F. Song, L. Li, H. Zhang, D. Y. Shen, D. Y. Tang, and K. P. Loh, Opt. Express **21**, 10010 (2013).
22. D. Y. Tang, L. M. Zhao, B. Zhao, and A. Q. Liu, Phys. Rev. A **72**, 43816 (2005).
23. D. Y. Tang, B. Zhao, L. M. Zhao, and H. Y. Tam, Phys. Rev. E **72**, 16616 (2005).